

Interdecadal Sea Level Fluctuations at Hawaii

YVONNE L. FIRING, MARK A. MERRIFIELD, THOMAS A. SCHROEDER, AND BO QIU

School of Ocean and Earth Science and Technology, University of Hawaii at Manoa, Honolulu, Hawaii

(Manuscript received 6 October 2003, in final form 4 May 2004)

ABSTRACT

Over the past century, tide gauges in Hawaii have recorded interdecadal sea level variations that are coherent along the island chain. The generation of this signal and its relationship to other interdecadal variability are investigated, with a focus on the last decade. Hawaii sea level is correlated with sea surface height (SSH) over a significant portion of the North Pacific Ocean, and with the Pacific–North America (PNA) index, which represents teleconnections between tropical and midlatitude atmospheric variations. Similar variations extend well below the thermocline in World Ocean Atlas temperature. Comparison with NCEP reanalysis wind and pressure shows that high (low) sea level phases around Hawaii are associated with an increase (decrease) in the strength of the Aleutian low. The associated wind stress curl pattern is dynamically consistent with observed sea level anomalies, suggesting that sea level at Hawaii represents large-scale changes that are directly wind-forced in concert with the PNA. Atmospheric modulation, as opposed to Rossby wave propagation, may explain the linkage of Hawaii sea level to North American sea level and ENSO events. A wind-forced, baroclinic Rossby wave model replicates some aspects of the interdecadal SSH variations and their spatial structure but fails to predict them in detail near Hawaii. The accuracy of wind products in this region and over this time period may be a limiting factor. Variations in mixed layer temperature due to surface heat flux anomalies may also contribute to the interdecadal sea level signal at Hawaii.

1. Introduction

Hourly tide gauge measurements have been collected in Hawaii for nearly a century, providing one of the longest oceanographic time series in the Pacific Ocean (Fig. 1). The time series provide a unique record of ocean variability in the central region of the subtropical gyre. Present in all Hawaii tide gauge records is an interdecadal fluctuation with 10–25-yr time scales and peak-to-trough changes of ~ 5 cm (Fig. 1). Polovina et al. (1994) showed that similar variability occurs along the North American coast in San Francisco and San Diego, California, tide gauge records (Fig. 2). Isotherm displacements measured between Hawaii and California show similar fluctuations, suggesting a connection with large-scale circulation changes in the eastern Pacific. While the decadal fluctuations are qualitatively similar at the three stations, cross correlations are generally low, because the relative timing of events is not consistent. For example, the high sea level event in the 1980s occurs at Honolulu, Hawaii, before San Francisco, whereas in the 1940s and 1960s Honolulu lags San Francisco.

Along the North American coast, the decadal variations appear to be linked closely to higher-frequency

ENSO events. For instance, the high sea level at San Diego and San Francisco during the 1980s is centered about the 1982–83 El Niño, and the subsequent low is centered about the 1987 La Niña. While the connection is obvious along the coast (see also Enfield and Allen 1980; Chelton and Davis 1982), at Hawaii the ENSO signal is not as apparent. Yet the amplitude of the decadal signal is similar at the three locations. It is tempting to ascribe the Honolulu signal to Rossby waves that originate at the eastern boundary during ENSO events and propagate westward to Hawaii. Sturges (1987) noted a coherence between San Francisco and Honolulu sea level at 5–8-yr periods with a phase suggestive of Rossby wave propagation. Jacobs et al. (1994) saw ENSO-related Rossby waves in *Geosat* altimeter data. Miller et al. (1997) found wave propagation associated with ENSO southward of 30°N in XBT observations. The features propagate across the Pacific basin at speeds higher than theoretical Rossby wave speeds. In terms of Hawaii sea level, wave propagation does not explain why decadal events sometimes occur earlier at Hawaii than at California (e.g., the high event in the early 1980s; Fig. 2).

The importance of wind-forced Rossby waves to North Pacific sea surface height (SSH) variations has been considered by Fu and Qiu (2002). Their simple two-layer model used wind stress curl from the National Centers for Environmental Prediction (NCEP)–National

Corresponding author address: Yvonne Firing, Department of Oceanography, University of Hawaii at Manoa, 1000 Pope Road, Honolulu, HI 96822.
E-mail: firing@hawaii.edu

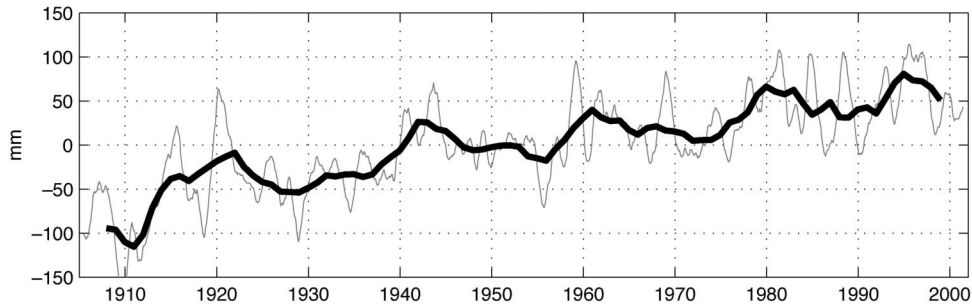


FIG. 1. Honolulu sea level referenced to an arbitrary benchmark on land. The thin line shows annual means, and the thick line shows 5-yr means.

Center for Atmospheric Research (NCAR) reanalysis to force Ekman pumping and mode-1 Rossby waves. The result described a significant portion of the Ocean Topography Experiment (TOPEX)/Poseidon (T/P) variability north of 30°N ; however, the model results were not significantly correlated with observations between 20° and 30°N , the latitude range of the Hawaiian Islands. Inclusion of a boundary-forced component did not improve the model skill other than adjacent to the boundary. Kawabe (2000) modeled Honolulu sea level using wind-forced baroclinic and barotropic Rossby waves. The simulation only accounted for $\sim 16\%$ of the observed variance at Honolulu, consistent with the results of Fu and Qiu (2002). Lysne and Deser (2002) found good correlations between Ekman pumping (from NCEP reanalysis wind stress curl) and thermocline anomalies in several regions of the Pacific, none of which include Hawaii. They also found evidence of

propagation but noted that correlations often decay within 20° – 30° . Leonardi et al. (2002) used the Naval Research Laboratory Layered Ocean Model (NLOM) to investigate variability in the subtropical northeast Pacific (10° – 30°N , 90° – 150°W). At interannual time scales, the dominant response is attributed to large-scale wind stress curl variations acting through Ekman pumping. The wind-forced Rossby wave response propagated westward at about 2 times the theoretical speed. In addition, freely propagating Rossby waves originating from the eastern boundary were evident on biennial time scales. Leonardi et al. (2002) note a decadal-scale response in the NLOM simulations, but the model runs were too short to fully investigate this response.

Given the length of Hawaii sea level records, it is of interest to know what aspect of Pacific interdecadal fluctuations they represent. We will consider the following indices, which measure such variability and have some connection to ENSO. The Southern Oscillation index (SOI) represents interannual and decadal ENSO variations in the Tropics. The Pacific–North America (PNA) index (Horel and Wallace 1981; Wallace and Gutzler 1981) represents atmospheric teleconnections between ENSO and the midlatitudes and contains significant interdecadal components. EOFs of upper-ocean heat content are correlated with both ENSO and the PNA (Deser et al. 1996), suggesting the probability of a similar connection with sea level.

In this paper, we find that sea level fluctuations at Hawaii are correlated with SSH, dynamic height, and winds over the northeast Pacific, with spatial patterns consistent with dominant modes of interdecadal variability. Low-frequency modulations of the wind field near and to the east of Hawaii seem to drive the interdecadal sea level signal. Attempts to simulate wind-forced changes in Hawaii sea level with a simple Rossby wave model, however, are inconclusive. In particular, heat changes in the upper 100 m, which were not simulated, may also account for a portion of the signal.

We begin by describing the data used in this study and some of the processing methods (section 2). The spatial extent of the Hawaii signal is considered in section 3 using altimeter and hydrographic data. Related

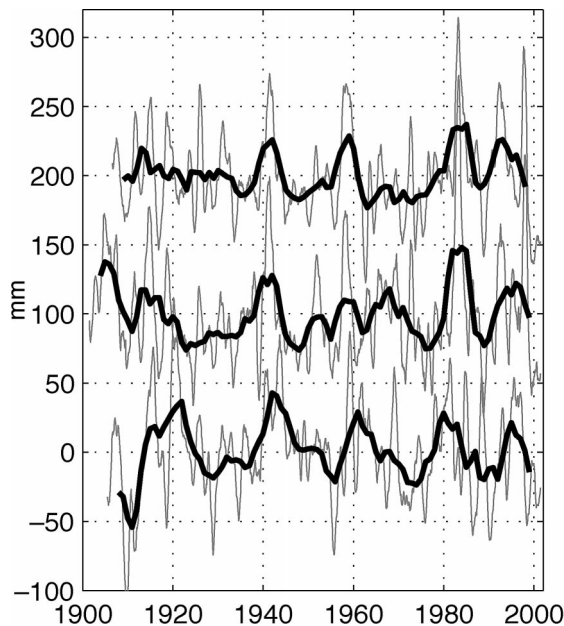


FIG. 2. Sea level at (top to bottom) San Diego, San Francisco, and Honolulu; thin lines are smoothed annual means and thick lines are 5-yr means. A linear trend was removed from each time series.

changes in atmospheric pressure and wind stress are described in section 4, and the results are discussed in section 5.

2. Datasets and methods

Tide gauge data, collected by the National Ocean Service (NOS), were obtained from the University of Hawaii Sea Level Center in the form of monthly means. The detrended Hawaii sea level time series (from Hilo, Kahului, Honolulu, and Nāwiliwili) are highly correlated and all exhibit similar decadal variability. To emphasize this regionally coherent signal, the linear trend and annual cycle were removed from the time series and an EOF analysis was performed. The first mode explains 90% of the total variance and is highly correlated (0.96) with Honolulu sea level. This mode-1 time series, referred to here as Hawaii sea level, extends back to 1955; the Honolulu time series is used to represent Hawaii sea level prior to this date. The other NOS tide gauge time series examined are from Midway Island, San Diego, and San Francisco (Figs. 2 and 4). All sea level records have been corrected for the inverse barometer effect using monthly NCEP reanalysis sea level pressure.

TOPEX/Poseidon and Jason altimeter SSH from late 1992 through early 2003 was obtained from G. Mitchum of the University of South Florida. The data are processed to a 1° grid at approximately 10-day intervals and are pressure-corrected (for a complete description, see Lagerloef et al. 1999). Hydrographic data are provided by the Hawaii Ocean Time-Series (HOT) program and consist of quasi-monthly CTD data from two sites, located about 4 km west and 100 km north of Oahu. Data from late 1988 through 2001 were interpolated to a monthly grid and put through a low-pass filter as described below, and the two stations were combined by averaging the data; dynamic height was computed relative to 1000 m.

The World Ocean Atlas (WOA) annual temperature anomalies for the time period 1948–95 were also used. The data extend to 500 m on a 1° grid; see Levitus et al. (2000). This product, obtained online from the National Oceanic and Atmospheric Administration (NOAA) Ocean Climate Laboratory (OCL) Web site at <http://www.nodc.noaa.gov/OC5>, is based on a dataset that is sparse in both space and time, especially outside of established shipping routes. The WOA data are used to support the findings obtained from the satellite SSH and the HOT hydrographic data.

NCEP reanalysis sea level pressure and surface wind stress from 1948 on (Kalnay et al. 1996) were provided by the NOAA–Cooperative Institute for Research in Environmental Sciences (NOAA–CIRES) Climate Diagnostics Center (CDC), Boulder, Colorado, from their Web site at <http://www.cdc.noaa.gov>. World Ocean Circulation Experiment (WOCE) monthly scatterometer wind stress from early 1992 to mid 2000 was obtained from the Institut Francais pour l'Exploitation de la Mer

(IFREMER). Reynolds, Stokes, and Smith NOAA Version-2 Optimum Interpolation SST from 1981 to the present and reconstructed SST data from 1950 through 1999 were provided by the NOAA–CIRES CDC.

Low-frequency time series were generated by removing an annual harmonic and applying 1- and 5-yr (to emphasize the decadal signal) running mean filters. A Gaussian filter was used for the 1-yr average and a boxcar filter was used for the 5-yr average (to reduce data loss at the ends of the time series). The results presented in this study are not sensitive to the low-pass-filter function.

3. Horizontal and vertical structures

To examine the spatial extent of the interannual sea level fluctuations observed at Hawaii, we regress and correlate the T/P SSH on the Hawaii time series. The regression (at zero lag) shows that the Hawaii record represents sea level changes over a large portion of the northeast Pacific (Fig. 3).

The Hawaiian Islands are located in the southern arm of a broad horseshoe-shaped area of positive regression coefficients that extends along the North American coast to Alaska. In the center of this pattern, SSH fluctuates 180° out of phase with SSH at Hawaii. Correlations are similar, and the same pattern appears in the dominant EOF mode of T/P SSH [not shown here; see Fig. 4 in Qiu (2002)]. A comparison of tide gauge records at Midway ($28^\circ 13'N$, $177^\circ 22'W$) and the main Hawaiian Islands shows a negative correlation (Fig. 4), consistent with the SSH pattern in Fig. 3.

Figure 3 was derived from approximately 10 years of data, or a single decadal cycle. To investigate the persistence of this pattern, we use WOA temperature anomalies for the period 1948–95. Dynamic height (0/500 m) is computed using time-varying temperature and a constant salinity profile. The zero-lag regression of the dynamic height on Hawaii sea level (Fig. 5) resembles Fig. 3. The regression patterns obtained using 1- and 5-yr running averages are similar, suggesting that the pattern represents variability at both interannual and decadal time scales. The first of two notable differences between Figs. 3 and 5 is in the southeast where the dynamic height regression is positive and the sea level regression is negative. The other is in the Gulf of Alaska and south of the Aleutians where the sea level regression shows strong positive values, which in the dynamic height regression are limited to the coast by a more extensive central negative region. These differences could be due to the different time periods, to the exclusion of variability below 500 m in the dynamic height data, or to the quality of the temperature data coverage. Because the regression amplitudes near Hawaii are high in both cases, however, it appears that most of the variability in decadal sea level can be ascribed to temperature variability in the upper 500 m. Deser et al. (1996) found a decadal-scale spatial pattern similar to that of

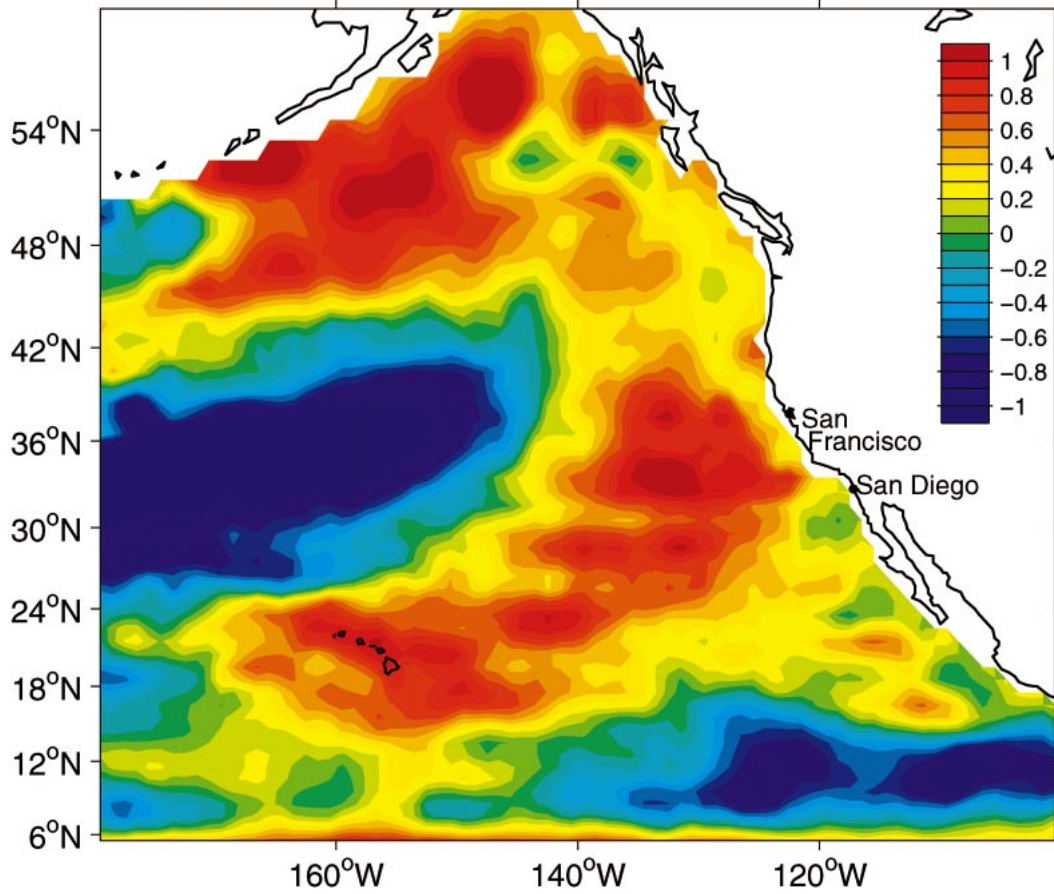


FIG. 3. Regression (at zero lag) of T/P sea surface height anomaly on Hawaii sea level. The data have been smoothed with an annual Gaussian filter.

Fig. 5 in the upper-400-m WOA data from 1970 to 1991. A regression covering only the time period 1970–95 (not shown) produces stronger values in most positive areas but an almost identical spatial pattern.

The zero-time-lag regression analysis does not pro-

vide information about the phase of the signal. For example, a westward-propagating Rossby wave could account for the progression from positive to negative regression values seen at midlatitudes. Hovmöller diagrams are used to examine the phase characteristics of

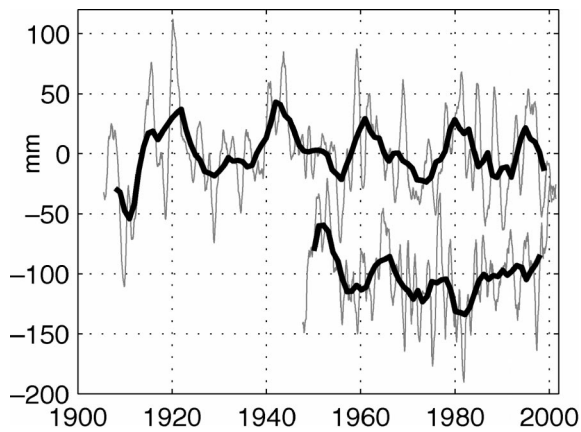


FIG. 4. Sea level at (top to bottom) Honolulu and Midway; thin lines are smoothed annual means, and thick lines are 5-yr means. A linear trend was removed from each time series.

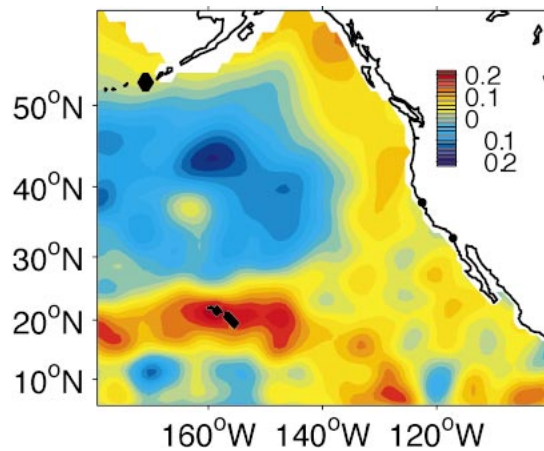


FIG. 5. Regression of annual mean dynamic height (0/500 m) from WOA on Hawaii sea level.

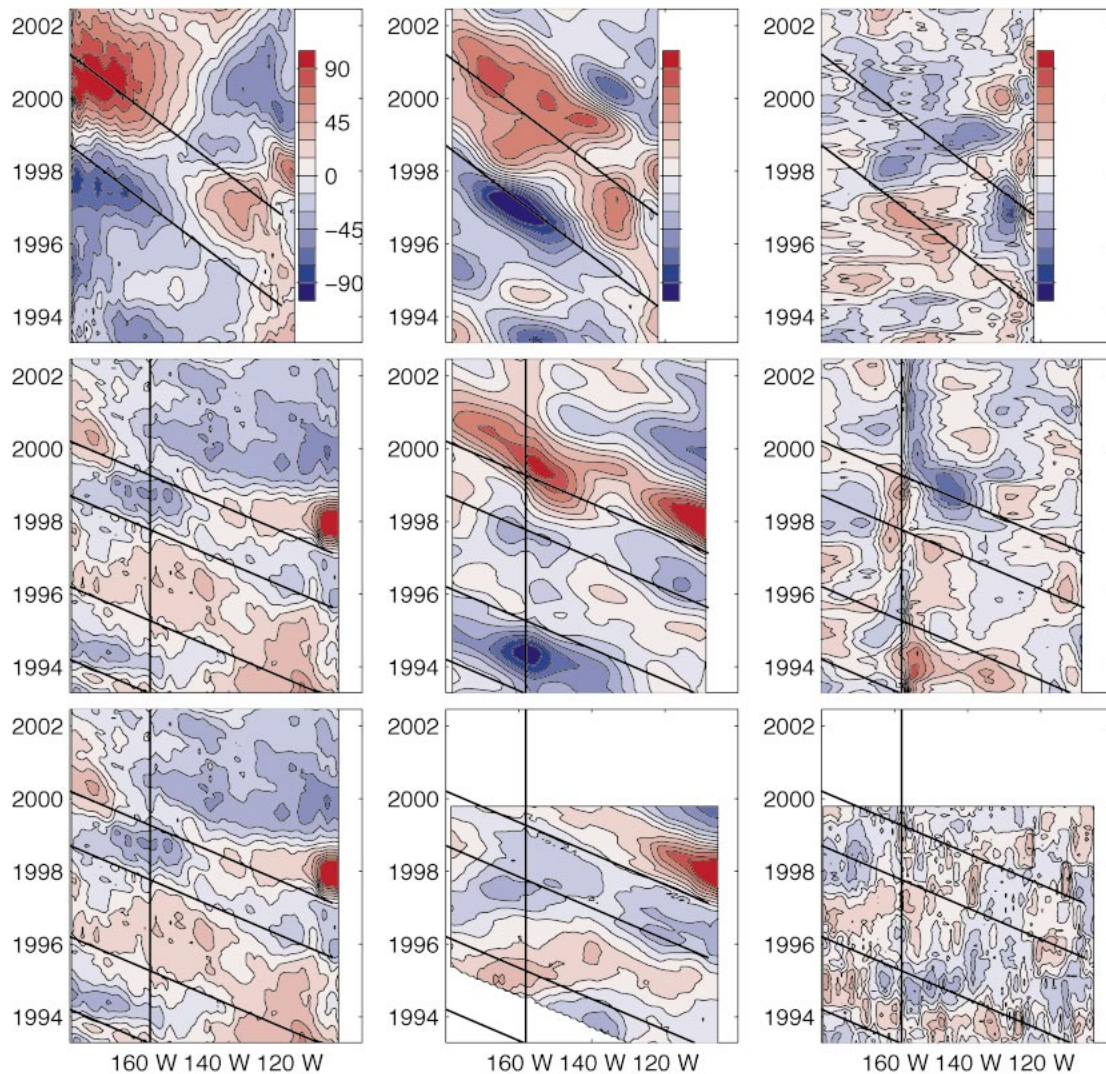


FIG. 6. Hovmöller diagrams of (left) T/P sea level, (center) wind stress curl-forced sea level model, and (right) wind stress curl at (top) 34°N and (center and bottom) 21°N ; top two panels use NCEP and bottom uses WOCE. The scaling of wind stress curl and modeled sea level is arbitrary. The vertical lines at 21°N indicate the approximate longitude of Oahu, while the other lines show the theoretical speed of mode-one baroclinic Rossby waves.

the variability and to identify the nature and extent of propagation. At 34°N (Fig. 6), in the center of the horseshoe pattern, the change from low to high sea level anomaly in the western part of the region occurs nearly simultaneously with an opposite-signed sea level change in the east. Although the high sea level events occur along a mode-1 Rossby wave characteristic, they are separated by a brief low (in 1998 near 150°W). Likewise, the low sea level event in the east does not propagate into the western region. The sea level changes are nearly 180° out of phase east and west of 150°W , similar to a standing wave. This is in keeping with the observations of Miller et al. (1997) that ocean temperature variability north of 30°N is based on a combination of direct forcing (through wind stress curl variations) and

westward propagation. Propagation is more apparent at the latitude band of Hawaii (21°N). The high sea level that occurs at Hawaii in 1996, and possibly the low sea level event that follows, appear to have propagated from the east at speeds consistent with a mode-1 Rossby wave. Lagged correlations (not shown) between T/P SSH at Hawaii and locations farther east, however, do not indicate dominant westward propagation; the highest correlations occur near zero time lag and extend to 150°W . A Hovmöller diagram of steric height at 21°N (from WOA temperature; not shown) shows a mix of propagating and nonpropagating events for the period from 1945 through 1995.

Another issue related to Rossby waves is whether SSH variations along the North America coast, primarily as-

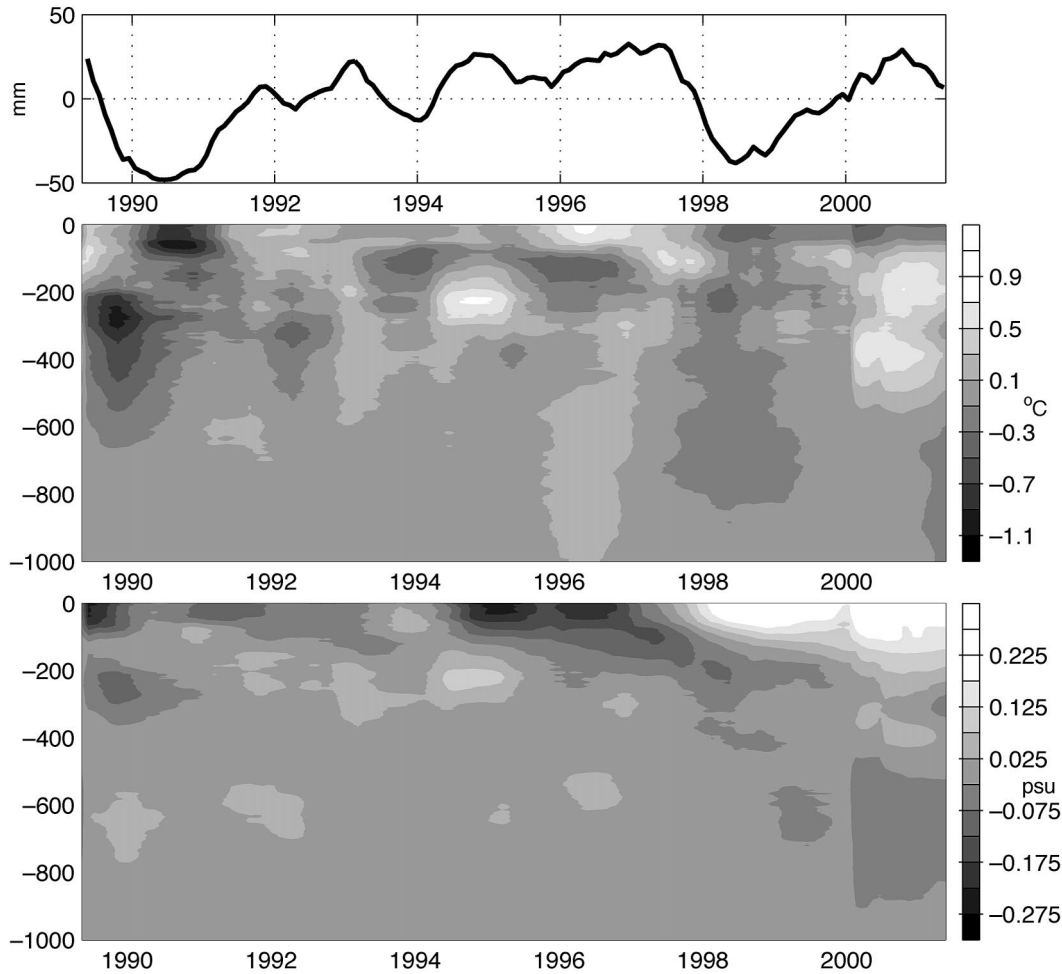


FIG. 7. Dynamic height (0/1000 m), temperature anomalies, and salinity anomalies at HOT. Data were smoothed using a Gaussian annual mean filter.

sociated with ENSO, propagate westward to reach Hawaii. The coastal high sea level event associated with the 1997–98 El Niño does not appear to have generated propagating signals at either 21° or 34°N. At 21°N a band of high sea level reaches offshore during the El Niño event, but, in contrast to reports on previous El Niños, the event is nonpropagating. We will consider wind forcing and Rossby wave propagation in section 4.

The vertical structure of temperature and salinity associated with the interannual sea level variations is investigated using the HOT data. The interannual dynamic height computed from the HOT data is highly correlated (0.86) with Hawaii sea level, capturing the decadal high in the mid-1990s (Fig. 7). This signal is associated with temperature changes in the main thermocline (250-m depth) of up to $\pm 0.6^{\circ}\text{C}$ and isotherm displacements below the thermocline of ± 50 m. Approximately 75% of the surface dynamic height variance can be accounted for by temperature changes between 50 m [approximately the base of the mixed layer; Karl et al. (1995)]

and 500 m. The surface mixed layer accounts for approximately 25% of the variance. The mixed layer contribution is consistent with the correlation between Hawaii sea level and local SST during the 1990s (0.79). The WOA dynamic height near Hawaii has a smaller contribution from the mixed layer ($\sim 10\%$), and the correlation between sea level and SST is only 0.41 over the longer time period. This may reflect either data sampling issues and/or a real change during the 1990s of the role of the mixed layer in determining the dynamic height. Although interannual salinity variations are substantial in the HOT area (Lukas 2001), their effects on dynamic height at the decadal time scale, at least in the 1990s, are minimal, justifying our use of a climatological profile in computing dynamic height from WOA temperature.

The thermocline changes observed at HOT do not exhibit downward propagation suggestive of subduction like that observed by Deser et al. (1996) in WOA data for a region north of Hawaii. Cold anomalies at Hawaii

might be associated with waters that spread southward from the subduction region; however, we note that the temperature changes at HOT extend to 1000 m in some cases, well below the depths of subducted waters identified by Deser et al. (1996). In addition, it is not clear how deep warm anomalies at HOT could result from this subduction process.

4. Relationship to atmospheric variability

Hawaii sea level is compared with regional atmospheric patterns by forming composites of surface winds and pressure during decadal high and low sea level events at Hawaii. The composites are obtained for December through February, because it has been observed that interannual variations in this region are dominated by changes in winter conditions (e.g., Namias et al. 1988). The two main features in this area are the North Pacific high, centered near 30°N, 230°E, and the Aleutian low to the northwest (Fig. 8). During high sea level years at Hawaii, the Aleutian low is stronger, and the North Pacific high is weaker, than in low sea level years. This is accompanied by a cyclonic wind anomaly between 40° and 50°N with a slight weakening of the northeast trades near Hawaii. A region of strong positive wind stress curl anomaly develops between the Aleutian low and North Pacific high, while weak negative curl anomalies occur south of 30°N. The opposite occurs during periods of low Hawaii sea level. The composites were constructed using NCEP reanalysis winds; however, similar results are obtained for the recent WOCE satellite wind product.

The atmospheric patterns described above, and their relationship to sea surface temperature and upper-ocean heat content, are well documented (e.g., Namias et al. 1988; Deser and Blackmon 1995, Polovina et al. 1995, Miller et al. 1998). Deser and Blackmon (1995) identified two modes of SST variability, an ENSO mode and a North Pacific mode, the latter of which resembles both the Pacific–North America pattern of Wallace and Gutzler (1981) (derived from 500-hPa atmospheric pressure level), and our regression patterns. Figure 9 compares the SOI and PNA index with Hawaii sea level. At interannual time scales, the correlations with both indices are weak (-0.14 and 0.25). At interdecadal time scales, the SOI is still weakly correlated with Hawaii sea level (-0.39), while the PNA has a stronger correlation (0.71). The high correlation with the PNA follows from the correspondence between Hawaii sea level and large-scale sea level pressure and winds discussed above (Fig. 8). Comparison with the Aleutian low pressure index (Beamish et al. 1997, not shown), which is similar to the PNA index but has a longer record (1905–2001), gives a correlation of 0.40 .

The correspondence between Hawaii sea level and the PNA index suggests that decadal fluctuations in Hawaii sea level are forced by weak southern extensions of the large-scale atmospheric pattern associated with

the Aleutian low. The wind stress curl anomaly pattern matches the sea level regression pattern (Fig. 3). In the absence of friction, local wind stress curl forcing should coincide with the rate of change of sea level through Ekman pumping. The connection between Hawaii sea level and wind forcing must also account for Rossby wave propagation effects.

To examine the influences on Hawaii sea level of the interior wind stress curl forcing and the boundary forcing due to sea level changes along the North American coast, we consider the simple model of Fu and Qiu (2002), described above. Fu and Qiu (2002) have modeled interannual sea level fluctuations in the North Pacific, finding that the best correlations with T/P observations occur at higher latitudes than Hawaii. Near Hawaii, their model accounted for less than 20% of the T/P-measured SSH variability. The inclusion of the boundary forcing did not significantly improve these results. We adopt the model and, instead of the interannual variations sought by Fu and Qiu (2002), compare the results with the long Hawaii record, with an emphasis on capturing the decadal sea level high in the mid-1990s. The model is forced using NCEP reanalysis wind stress or WOCE wind stress, and sea level at the eastern boundary is specified using T/P data. The propagation speeds of mode-1 baroclinic Rossby waves are estimated using the Rossby radii given by Chelton et al. (1998). A Newtonian decay factor of 9% per month is used to account for Rossby wave dissipation. The decay factor and the relative magnitude of the boundary condition were adjusted to best reproduce the observed variability; amplitude was not considered.

The model–data comparison in the 1990s is shown in the form of Hovmöller diagrams (Fig. 6). The main feature of interest is the high sea level event in the mid-1990s at Hawaii. The NCEP-forced model does not produce this event and predicts a high event in 2000 that is not evident in the T/P data. The model–data comparisons are better near the eastern boundary, but this is due primarily to the inclusion of the T/P boundary condition. The best decay factor is 9% per month, or about 90% in two years, about the time it would take a mode-1 Rossby wave to get from the coast to Hawaii. We note that weak- or no-decay runs led to the worst results, consistent with the findings of Lysne and Deser (2002) in regard to correlations between thermocline depth anomalies along Rossby wave characteristics. Over the longer term (1955–2002), the correlation between 5-yr running means of predicted and observed Hawaii sea level is 0.31 (Fig. 10). Kawabe (2000) obtained similar results, even with the inclusion of the barotropic and second baroclinic modes. At 34°N, the model corresponds more closely to T/P observations (Fig. 6 top panel), as was found by Fu and Qiu (2002). The observed high and low features at 34°N are present in both simulations. The importance of the decay factor was even more noticeable at this latitude than at Hawaii, emphasizing that the sea level variability is associated

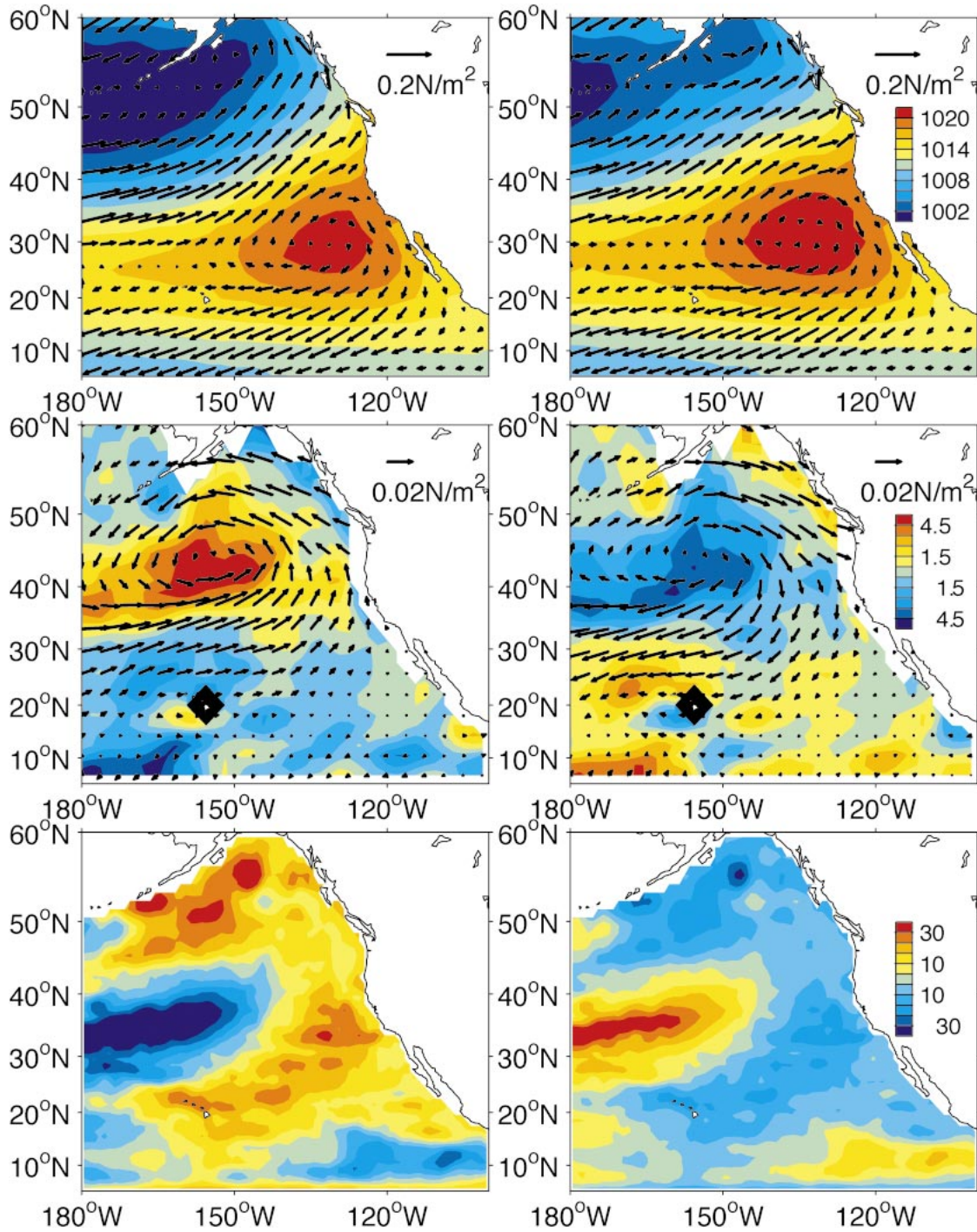


FIG. 8. Composites from years in which Hawaii sea level was (left) high and (right) low: (top) winter wind stress and sea level pressure, (middle) winter wind stress anomaly and wind stress curl anomaly, and (bottom) SSH.

more with direct or nearby wind forcing than with freely propagating Rossby waves.

The model was also forced with the WOCE wind stress to determine if the satellite wind product could give a better prediction. The WOCE winds are only

available between 1992 and 2000. The correlation with Hawaii sea level is improved (0.63); in particular, the mid-1990s high and following low are reproduced using the WOCE winds. The high event in the model is associated only with nearby wind forcing; in contrast, the

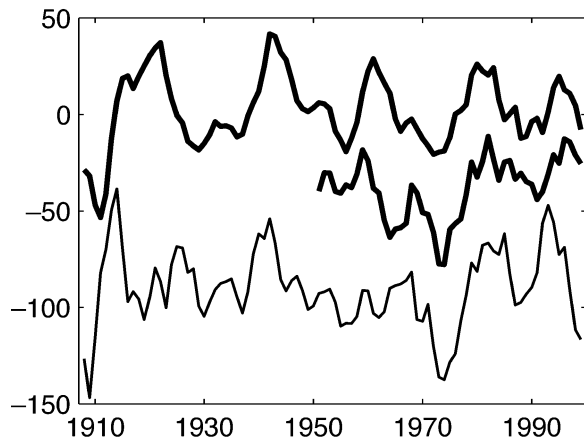


FIG. 9. Five-year means of (top to bottom) Hawaii sea level (linear trend removed), PNA index, and SOI. Indices are scaled to match Hawaii sea level (mm).

observed event appears to have propagated across the basin. Inspection of the wind stress curl maps (Fig. 8) shows considerable differences between the two wind products, the largest of which occur just east of Hawaii. Auad et al. (2001) found low correlations between NCEP and Comprehensive Ocean–Atmosphere Dataset wind stress anomalies in this region. Lysne and Deser (2002) also describe discrepancies between historic Pacific wind products.

We note that the two-layer model does not include mixed layer dynamics, which may help to explain the poor model results for Hawaii's latitude. At the HOT sites, temperature changes in the mixed layer account for approximately one-quarter of the dynamic height (0/1000 dbar) signal. In addition, both SST (not shown) and mixed layer temperature (Polovina et al. 1995) contain spatial patterns similar to that shown in Fig. 3. Cayan (1992) has shown that heat flux anomalies in the extratropical North Pacific are influenced by both wind speed and direction and are correlated with large-scale atmospheric circulation patterns. The combined effect of wind stress curl and mixed layer heat variations was assessed by a multiple linear regression of NCEP wind stress curl and SST, as a proxy for mixed layer heat, on 5-yr running mean Hawaii sea level. The regression accounted for only 9% of decadal Hawaii sea level variability, similar to the Rossby wave model result. During the 1990s, the regression model accounted for 64% of the interannual Hawaii sea level variability; however, the observed and predicted time series are dominated by one cycle of the decadal signal, and so it is difficult to determine the statistical significance of this result. Conversely, the model skill over this short time period may reflect the improved quality of wind stress and SST products due to satellite data.

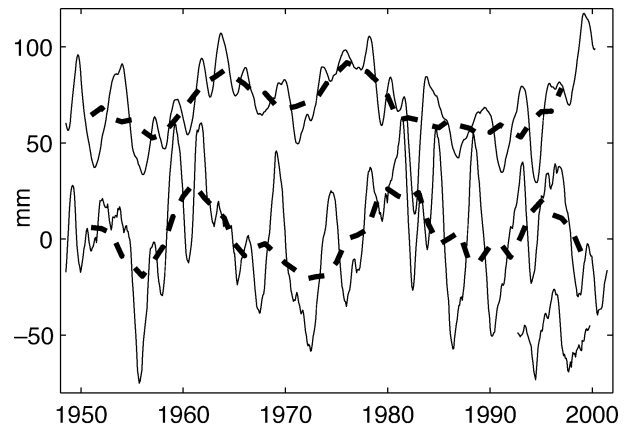


FIG. 10. Sea level anomalies at Hawaii (top to bottom) predicted from NCEP reanalysis wind stress curl, observed, and predicted from WOCE wind stress curl. Solid lines were smoothed using an annual Gaussian filter; dashed lines are 5-yr running means.

5. Summary and discussion

Interdecadal fluctuations in the North Pacific have been studied extensively, but usually in the context of SST and atmospheric variables or recent SSH changes observed by satellite altimeter. In this study, we have attempted to place the long time series of in situ sea level measurements at Hawaii into this framework and to examine the dynamics behind its variability. The primary results follow.

- 1) Interdecadal sea level fluctuations at Hawaii are part of a distinctive pattern in SSH and dynamic height that spans much of the northeast Pacific. Fluctuations at Hawaii are of the same sign as those along the North American coast. The relatively long sea level records at Midway, San Francisco, and San Diego provide in situ validation for this often-seen pattern.
- 2) HOT CTD data for the past decade indicate that interannual Hawaii sea level fluctuations are associated with temperature changes in the upper 1000 m. One-quarter of the dynamic height variability (0/1000 m) is contributed by the upper 50 m, and nearly three-quarters are contributed between 50 and 500 m.
- 3) High sea level at Hawaii is associated with weakened winter trade winds and a negative wind stress curl anomaly. These local atmospheric fluctuations are connected to large-scale changes centered north of Hawaii between 40° and 50°N.
- 4) Interdecadal Hawaii sea level is well correlated (0.71) with the PNA index, suggesting an indirect relationship with tropical variability. Correlation with the SOI is comparatively weak (−0.39).
- 5) Although a correlation exists between regional wind stress and Hawaii sea level, the dynamical relationship could not be resolved using a two-layer model combining local wind-forced Ekman pumping and mode-1 Rossby wave propagation. When forced by

NCEP wind stress, this model explained only ~10% of Hawaii sea level variability. WOCE wind forcing, based on satellite observations, produced better results than NCEP, but over a time period too short to evaluate significance for the decadal signal.

- 6) An attempt to assess the contribution of mixed layer heat content to Hawaii sea level variability using only SST was inconclusive.

Further modeling work in this area will require a careful assessment of atmospheric products. NCEP reanalysis wind stress curl did not replicate the interdecadal sea level signal at Hawaii. Historic wind products in the subtropical northeast Pacific may be insufficient for quantitative studies of wind forcing. WOCE satellite winds are too short for interdecadal comparisons, but they do give better results than NCEP, suggesting that more accurate wind products are required to determine the relative importance of local and remote wind forcing. We did not attempt to include directly the effects of surface heat flux because we found that products differed in this region and were not correlated with sea level changes at Hawaii. Smith et al. (2001) also found significant differences between NCEP reanalysis and observed heat fluxes. Auad et al. (2001) note that the correspondence is particularly poor at decadal time scales.

We began by noting the similarities among interdecadal sea-level time series from Honolulu, San Francisco, and San Diego (Fig. 2) and the correspondence between interdecadal highs and El Niño events, especially along the North American coast. All three stations lie within the region where interdecadal sea level changes occur approximately in phase (Figs. 3 and 5), apparently because of large-scale atmospheric changes. However, while San Francisco and San Diego sea levels are also influenced directly by ENSO through coastal-trapped waves (e.g., Enfield and Allen 1980; Chelton and Davis 1982), Hawaii is not. Hawaii's connection to ENSO comes through local atmospheric forcing teleconnected to the tropical variability, rather than as a result of wave propagation. The Hawaii–North America connection is primarily through common atmospheric forcing related to the PNA. Our attempt to model sea level changes due to this forcing was inconclusive at Hawaii; however, we believe that longer scatterometer time series will establish that wind stress curl forcing just to the east of Hawaii has the greatest influence on decadal fluctuations at Hawaii.

Acknowledgments. This work was supported by the National Aeronautics and Space Administration (961451) and the Office of Global Programs, National Oceanic and Atmospheric Administration (NA17RJ1230). Special thanks are extended to Dr. Jeffrey Polovina of the National Marine Fisheries Service and Dr. Gary Mitchum of FSU for numerous discussions and to Dr. Niklas Schneider of UH for his helpful suggestions.

REFERENCES

- Auad, G., A. J. Miller, J. O. Roads, and D. R. Cayan, 2001: Pacific Ocean wind stresses and surface heat fluxes from the NCEP reanalysis and observations: Cross-statistics and ocean model responses. *J. Geophys. Res.*, **106**, 22 249–22 265.
- Beamish, R. J., C. E. Neville, and A. J. Cass, 1997: Production of Fraser River sockeye salmon (*Oncorhynchus nerka*) in relation to decadal-scale changes in the climate and the ocean. *Can. J. Fish. Aquat. Sci.*, **54**, 543–554.
- Cayan, D. R., 1992: Latent and sensible heat flux anomalies over the northern oceans: The connection to monthly atmospheric circulation. *J. Climate*, **5**, 354–369.
- Chelton, D. B., and R. E. Davis, 1982: Monthly mean sea-level variability along the west coast of North America. *J. Phys. Oceanogr.*, **12**, 757–784.
- , R. A. deSzoeke, M. G. Schlax, K. E. Nagger, and N. Siwertz, 1998: Geophysical variability of the first baroclinic Rossby radius of deformation. *J. Phys. Oceanogr.*, **28**, 433–460.
- Deser, C., and M. L. Blackmon, 1995: On the relationship between tropical and North Pacific sea surface temperature variations. *J. Climate*, **8**, 1677–1680.
- , M. A. Alexander, and M. S. Timlin, 1996: Upper-ocean thermal variations in the North Pacific during 1970–1991. *J. Climate*, **9**, 1840–1855.
- Enfield, D. B., and J. S. Allen, 1980: On the structure and dynamics of monthly mean sea level anomalies along the Pacific Coast of North and South America. *J. Phys. Oceanogr.*, **10**, 557–578.
- Fu, L.-L., and B. Qiu, 2002: Low-frequency variability of the North Pacific Ocean: The roles of boundary- and wind-driven baroclinic Rossby waves. *J. Geophys. Res.*, **107**, 3220, doi:10.1029/2001JC001131.
- Horel, J. D., and J. M. Wallace, 1981: Planetary scale atmospheric phenomena associated with the Southern Oscillation. *Mon. Wea. Rev.*, **109**, 813–829.
- Jacobs, G. A., H. E. Hurlburt, J. C. Kindle, E. J. Metzger, J. L. Mitchell, W. J. Teague, and A. J. Wallcraft, 1994: Decade-scale trans-Pacific propagation and warming effects of an El Niño anomaly. *Nature*, **370**, 360–363.
- Kalnay, E., and Coauthors, 1996: The NCEP/NCAR 40-Year Reanalysis Project. *Bull. Amer. Meteor. Soc.*, **77**, 437–471.
- Karl, D. M., R. Letelier, D. Hebel, L. Tupas, J. Dore, J. Christian, and C. Winn, 1995: Ecosystem changes in the North Pacific subtropical gyre attributed to the 1991–92 El Niño. *Nature*, **373**, 230–234.
- Kawabe, M., 2000: Calculation of interannual variations of sea level in the subtropical North Pacific. *J. Oceanogr.*, **56**, 691–706.
- Lagerloef, G. S. E., G. T. Mitchum, R. B. Lukas, and P. P. Niiler, 1999: Tropical Pacific near-surface currents estimated from altimeter, wind, and drifter data. *J. Geophys. Res.*, **104**, 23 313–23 326.
- Leonardi, A. P., S. L. Morey, and J. J. O'Brien, 2002: Interannual variability in the eastern subtropical North Pacific Ocean. *J. Phys. Oceanogr.*, **32**, 1824–1837.
- Levitus, S., C. Stephens, J. Antonov, and T. P. Boyer, 2000: *Yearly and Year-Season Upper Ocean Temperature Anomaly Fields, 1948–1998*. NOAA Atlas NESDIS 40, 23 pp.
- Lukas, R., 2001: Freshening of the upper thermocline in the North Pacific subtropical gyre associated with decadal changes of rainfall. *Geophys. Res. Lett.*, **28**, 3485–3488.
- Lysne, J., and C. Deser, 2002: Wind-driven thermocline variability in the Pacific: A model–data comparison. *J. Climate*, **15**, 829–845.
- Miller, A. J., W. B. White, and D. R. Cayan, 1997: North Pacific thermocline variations on ENSO timescales. *J. Phys. Oceanogr.*, **27**, 2023–2039.
- , D. R. Cayan, and W. B. White, 1998: A westward-intensified decadal change in the North Pacific thermocline and gyre-scale circulation. *J. Climate*, **11**, 3112–3127.

- Namias, J., X. Yuan, and D. R. Cayan, 1988: Persistence of North Pacific sea surface temperature and atmospheric flow patterns. *J. Climate*, **1**, 682–703.
- Polovina, J. J., G. T. Mitchum, N. E. Graham, M. P. Craig, E. E. Demartini, and E. N. Flint, 1994: Physical and biological consequences of a climate event in the central North Pacific. *Fish. Oceanogr.*, **3**, 15–21.
- , —, and G. T. Evans, 1995: Decadal and basin-scale variation in mixed layer depth and the impact on biological production in the central and North Pacific, 1960–88. *Deep-Sea Res.*, **42**, 1701–1716.
- Qiu, B., 2002: Large-scale variability in the midlatitude subtropical and subpolar North Pacific Ocean: Observations and causes. *J. Phys. Oceanogr.*, **32**, 353–375.
- Smith, S. R., D. M. Legler, and K. V. Verzone, 2001: Quantifying uncertainties in NCEP reanalyses using high-quality research vessel observations. *J. Climate*, **14**, 4062–4072.
- Sturges, W., 1987: Large-scale coherence of sea level at very low frequencies. *J. Phys. Oceanogr.*, **17**, 2084–2094.
- Wallace, J. M., and D. S. Gutzler, 1981: Teleconnections in the geopotential height field during the Northern Hemisphere winter. *Mon. Wea. Rev.*, **109**, 784–812.